

# IL23R-Specific CAR Tregs for the Treatment of Crohn's Disease

Yue Cui,<sup>a, </sup> Marion David,<sup>a, </sup> Laura Bouchareychas,<sup>a</sup> Sandrine Rouquier,<sup>a</sup> Satria Sajuthi,<sup>b</sup> Marion Ayrault,<sup>a</sup> Candice Navarin,<sup>a</sup> Gregory Lara,<sup>a</sup> Audrey Lafon,<sup>a</sup> Gaëlle Saviane,<sup>a</sup> Sonia Boulakirba,<sup>a</sup> Alexandra Menardi,<sup>a</sup> Alexandra Demory,<sup>a</sup> Jihane Frikeche,<sup>a</sup> Stephanie de la Forest Divonne Beghelli,<sup>a</sup> Hsiaomei Heidi Lu,<sup>b</sup> Celine Dumont,<sup>a</sup> Tobias Abel,<sup>a</sup> David Fenard,<sup>a</sup> Maurus de la Rosa,<sup>a, #</sup> Julie Gertner-Dardenne<sup>a, #</sup>

<sup>a</sup>Research, Sangamo Therapeutics, Valbonne, France

<sup>b</sup>Bioinformatics, Sangamo Therapeutics, Richmond, CA, USA

Corresponding author: Julie Gertner-Dardenne, Research, Sangamo Therapeutics, Allée de la Nertière, 06560 Valbonne, France. Tel: +33 4 97 21 83 00; Email: [jgertnerdardenne@sangamo.com](mailto:jgertnerdardenne@sangamo.com); Yue Cui, Research, Sangamo Therapeutics, Allée de la Nertière, 06560 Valbonne, France. Email: [ycui@sangamo.com](mailto:ycui@sangamo.com)

#These authors have contributed equally to this work and share the last authorship.

## Abstract

**Background and Aims:** Regulatory T cells (Tregs) are key regulators in maintaining tissue homeostasis. Disrupted immune homeostasis is associated with Crohn's disease (CD) pathogenesis. Thus, Treg therapy represents a promising long-acting treatment to restore immune balance in the diseased intestine. Chimeric antigen receptor (CAR) T-cell therapy has revolutionized cancer treatment. This innovative approach also provides the opportunity to improve therapy for CD. By targeting a disease-relevant protein, interleukin-23 receptor (IL23R), we engineered Tregs expressing IL23R-CAR for treating active CD.

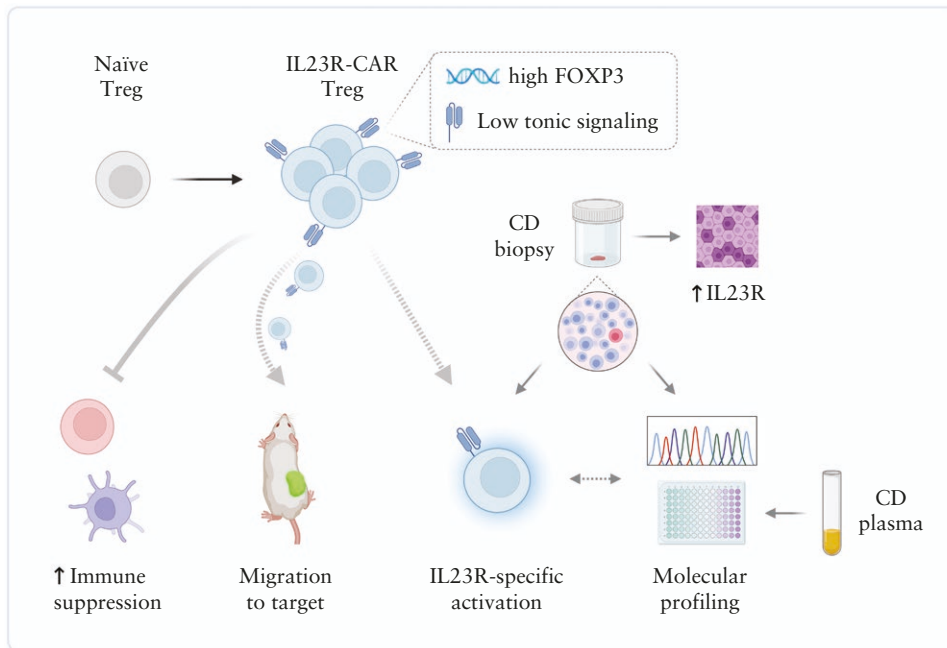
**Methods:** Intestinal IL23R expression from active CD was verified by immunohistochemical analysis. Phenotypic and functional characteristics of IL23R-CAR Tregs were assessed using *in vitro* assays and their migration capacity was monitored in a xenograft tumor model. Transcriptomic and proteomic analyses were performed to associate molecular profiles with IL23R-CAR Treg activation against colon biopsy-derived cells from active CD patients.

**Results:** Our study showed that IL23R-CAR displayed negligible tonic signaling and a strong signal-to-noise ratio. IL23R-CAR Tregs maintained regulatory phenotype during *in vitro* expansion, even when chronically exposed to proinflammatory cytokines and target antigen. IL23R engagement on IL23R-CAR Tregs triggered CAR-specific activation and significantly enhanced their suppressive activity. Also, IL23R-CAR Tregs migrated to IL23R-expressing tissue in humanized mice. Finally, IL23R-CAR Tregs elicited a specific activation against colon biopsy-derived cells from active CD, suggesting an efficient CAR engagement in active CD. Molecular profiling of CD patient biopsies also revealed transcriptomic and proteomic patterns associated with IL23R-CAR activation.

**Conclusions:** Overall, our results demonstrate that IL23R-CAR Tregs represent a promising therapy for active CD.

**Key Words:** CAR Treg; IL23R; Crohn's disease; cell therapy; IBD

## Graphical Abstract



## 1. Introduction

Crohn's disease (CD) is a chronic inflammatory bowel disease (IBD) of which most cases follow a relapsing and remitting pattern with a variable disease course and heterogeneous clinical outcome.<sup>1,2</sup> The pathogenesis of CD is driven by a range of genetic and environmental factors resulting in gut microbiota dysbiosis, disruption of the intestinal epithelial barrier, and aberrant host immune responses.<sup>2,3</sup> Despite recent advances in the development of biologics, including inhibitors of TNF- $\alpha$ ,  $\alpha 4\beta 7$ , and IL-12/23, there remains an unmet medical need, as not all patients respond uniformly to treatment and many patients lose response to treatment during the course of the disease.<sup>4,5</sup> Also, patients treated with biologics are at increased risk for developing opportunistic infections or malignancy.<sup>6</sup> Therefore, therapies offering long-lasting effects and tolerance induction with improved safety profiles are needed.

Regulatory T cells (Tregs), a subset of T lymphocytes that constitutively express the IL-2 receptor  $\alpha$  chain (CD25) and the transcription factor FOXP3, are key mediators of peripheral immune tolerance, particularly in the intestine.<sup>7,8</sup> In humans, impaired Treg/T effector balance has been associated with IBD development and progression.<sup>9,10</sup> Similarly, mice with deficient Treg activity are susceptible to severe colitis.<sup>11,12</sup> As such, substantial research in IBD has focused on immune regulation with Tregs, identified as cells holding therapeutic promise in this area.<sup>13–17</sup> CD45RA<sup>+</sup>CD4<sup>+</sup>CD25<sup>high</sup>T cells have been suggested as the most appropriate population for Treg therapy due to their homogeneity and phenotypic and functional stability upon *in vitro* expansion.<sup>18</sup> A later study demonstrated that *in vitro* expanded CD4<sup>+</sup>CD25<sup>+</sup>CD127<sup>lo</sup>CD45RA<sup>+</sup> Tregs have an epigenetically stable FOXP3 locus and are resistant to Th17 conversion. Importantly, these cells have the capacity to home to mucosal tissue, making them the most favorable population for Treg cell therapy for CD.<sup>19</sup>

Antigen-specific Tregs have been proven to be superior to polyclonal Tregs in controlling autoimmune diseases as demonstrated in murine models of diabetes,<sup>20</sup> multiple sclerosis,<sup>21</sup>

arthritis,<sup>22</sup> and colitis.<sup>23,24</sup> For the generation of antigen-specific Tregs, the use of a chimeric antigen receptor (CAR) has 2 major advantages: overcoming HLA restriction and increasing antigen specificity.<sup>25</sup> Built from an antibody-derived variable region linked to signaling and costimulatory domains of immune receptors,<sup>26</sup> CARs have been developed and successfully implemented in cancer treatments, with long-term remissions achieved in advanced-stage B-cell malignancies<sup>27–29</sup> and in neuroblastoma.<sup>30</sup> Recent preclinical studies have also shown the therapeutic potential of CAR Tregs to induce graft tolerance and to treat autoimmune diseases.<sup>31–41</sup> Our CAR-Treg platform exploits this concept by using a well-described signaling domain (CD3 $\zeta$  associated with CD28 costimulatory domain). Our manufacturing process allowed the expansion of stable (high expression of FOXP3) and persistent CAR Tregs.<sup>33,42</sup> The first-in-human study (NCT04817774) is currently ongoing to test CAR Tregs in renal transplantation. Encouragingly, intermediate results from the NCT04817774 study showed that CAR Tregs were well tolerated in the 6 patients dosed across 4 dose levels (personal communication). A second clinical study (NCT05234190) has also been initiated to assess CAR Tregs in liver transplantation.

The importance of IL-23 and its receptor IL23R in the pathogenesis of CD has been well established.<sup>43,44</sup> Genome-wide association studies identified that a loss of function mutation in the IL23R gene was protective against IBD.<sup>43</sup> In mouse colitis models, IL-23 drives inflammation and intestinal pathology, which can be reversed with an IL-23-blocking antibody.<sup>45–48</sup> Blockade of IL-12/23p40 or IL-23p19 has also been clinically validated for the treatment of IBD.<sup>44,49</sup> However, long-term treatment requires induction of tolerance, which may not be achieved by solely targeting the cytokine.

Hence, we developed a CAR to target IL23R and generated IL23R-CAR Tregs to investigate their potential for treating CD. Our study shows that the IL23R-CAR displays negligible tonic signaling and has a strong signal-to-noise ratio. IL23R-CAR Tregs maintain their regulatory phenotype

and exhibit target-dependent immunosuppression and immunomodulation. Importantly, IL23R-CAR Tregs elicit activation against colon biopsy-derived cells from CD. Overall, our study demonstrates that IL23R-CAR Tregs represent a potential therapeutic approach for treating CD. The molecular profiles associated with IL23R-CAR activation could also potentially support the development of biomarkers for clinical studies.

## 2. Methods

### 2.1. Cell lines

IL23R-expressing Jurkat cells were generated by overexpressing IL23R in Jurkat cells via a puromycin-selectable lentiviral vector. For the IL23R<sup>low</sup> Jurkat, the codon-optimized full-length sequence of human IL23R (UniProt #Q5VWK5) was tagged N-terminally with a 3x FLAG tag and placed upstream of a furin site, a self-cleavable T2A-peptide, and the sequence of the human IL12Rβ1 subunit. For IL23R<sup>high</sup> Jurkat, the extracellular domain of human IL23R was equipped with a Pepsin signal peptide, an N-terminal 3x FLAG tag, and was C-terminally fused to a PDGFR-transmembrane domain for increased cell surface expression. Jurkat cells were cultured in X-VIVO 15 media (Lonza). IL23R expression was monitored using anti-IL23R antibody staining and a FLAG tag (Supplementary Figure S3A, B).

### 2.2. Human cell preparation

Buffy coats were obtained from healthy volunteers via French Blood Establishment (Marseille, France). Peripheral blood mononuclear cells (PBMC) were isolated from buffy coat by density centrifugation using Ficoll-Paque (GE Healthcare). Biopsies from less or more affected areas were pooled individually and digested in RPMI 1640 media (ThermoFisher Scientific) containing 0.5 mg/mL type II collagenase (Sigma) at 37 °C and shaken for 30 minutes. Digested tissue was gently homogenized, and the released cells were harvested in a tube containing 10% v/v cold FCS and stored at 4 °C. The remaining tissue was subjected to a second incubation with RPMI 1640 media containing 1 mg/mL type II collagenase at 37 °C for 30 minutes. Digested tissue was gently homogenized, pooled with the cell suspension from the first digestion, filtered through a 100-μm cell strainer, and resuspended in X-VIVO 15 media (Lonza).

### 2.3. Preparation of IL23R-coated beads

IL23R-coated beads were prepared by coupling 5 mg Dynabeads (M-270 Epoxy, ThermoFisher Scientific) with 10 μg recombinant human IL23R Fc chimera protein (R&D Systems) using Dynabeads Antibody Coupling Kit (ThermoFisher Scientific), according to the manufacturer's instructions.

### 2.4. IL23R-CAR generation and lentiviral production

Anti-IL23R single-chain variable fragment (scFv) was identified by library screening. Anti-IL23R-scFv lead candidate was cloned into a lentiviral vector to generate IL23R-CAR, comprising a hinge domain, a transmembrane domain, and CD28-CD3ζ signaling domain. Control IL23R-ΔCAR is an IL23R-CAR lacking signaling domain. The CAR constructs were produced using a classical 4-plasmid lentiviral

system. Briefly, HEK293T cells were transfected with a third-generation lentiviral transfer vector expressing the CAR, the plasmid expressing HIV-1 gagpol (pMDLgpRRE), HIV-1 rev (pRSV.Rev), and the plasmid expressing the envelope glycoprotein of the vesicular stomatitis virus (pMD2.G). One-day post-transfection, viral supernatants were harvested, concentrated by centrifugation, aliquoted, and frozen at -80 °C for long-term storage. The infectious titers, expressed as the number of transducing units per milliliter (TU/mL), were obtained after transduction of Jurkat T cells with a serial dilution of viral supernatants, and transduction efficiency was evaluated after 3 days using flow cytometry.

### 2.5. Treg isolation, transduction, and expansion

Frozen Leukopaks were obtained from healthy volunteers via CliniSciences. Human Tregs and CD4<sup>+</sup>CD25<sup>-</sup> responder T cells (Tconv) were isolated from PBMC using EasySep Human CD4<sup>+</sup>CD127<sup>low</sup>CD25<sup>+</sup> Regulatory T Cell Isolation Kit (STEMCELL Technologies). Naïve CD4<sup>+</sup>CD127<sup>low</sup>CD25<sup>+</sup>CD45RA<sup>+</sup> Tregs were further purified by cell sorting and cultured in X-VIVO 15 (Lonza) or OpTmizer media (ThermoFisher Scientific) supplemented with 1000 U/mL recombinant human IL-2 (Proleukin) and anti-CD3/CD28 Dynabeads (ThermoFisher Scientific). Media containing IL-2 were replenished every 2-3 days. Tregs were transduced with lentiviral vectors at day 2, restimulated with anti-CD3/CD28 beads at day 7 and recovered at days 12-13 or transduced with lentiviral vectors at day 2 and recovered at days 9-11.

### 2.6. Treg chronic stimulation

After expansion, human naïve Tregs were stimulated with anti-IL23R-coated beads (1 Treg:1 bead) in the presence or absence of proinflammatory cytokines on day 15 and restimulated with the same condition on day 22. Cytokines were replenished every 2 days. The concentrations of cytokines were 1000 U/mL IL-2, 15 ng/mL IL-6, 10 ng/mL IL-1β, and 50 ng/mL TNFα.

### 2.7. Flow cytometry

Flow cytometry was performed with directly conjugated antibodies according to standard techniques and analyzed on MACSQuant Analyzer (Miltenyi Biotec), CytoFLEX (Beckman Coulter) flow cytometers, or SH800S Cell Sorter (Sony Biotechnology). All antibodies were purchased from Miltenyi Biotec unless otherwise stated. The antihuman antibody clones used included: CD4-VioBlue (VIT4), CD45RA-FITC (REA1047), CD127-APC (MB15-18C9), CD25-PE (STEMCELL Technologies, 2A3), CD4-VioGreen (REA623), CD69-APC or PE (REA824), GARP-PE (REA166), CD137-APC (REA 765), Helios-eF450 (eBioscience, 22F6), CD25-PE (REA570), CTLA-4-PE-Cy7 (BioLegend, BNI3), FOXP3-AlexaFluor647 (BD Biosciences, 259D/C7), CD127-APC-Vio770 (REA614), CD86-APC (REA968), HLA-DR-VioBlue (REA805), CD80-PE (REA661), and CD40-APC-Vio770 (REA733). FcR blocking reagent was used prior to surface marker staining. Dead cells were excluded using DAPI, PI, 7-AAD, or fixable viability dye. Staining for intracellular markers was performed using the FOXP3 Staining Buffer Set (Miltenyi Biotec). Intracellular IL-17A (BD Biosciences, N49-653) was measured following 4 hours of stimulation with PMA at 10 ng/ml, ionomycin at 1 μg/ml (Sigma), and GolgiStop (BD Biosciences). Cell proliferation was measured using cell proliferation dye eF450 (ThermoFisher Scientific).

IL23R-CAR was detected using anti-IL23R-scFv Klickmer (Immudex) or GFP reporter.

## 2.8. FOXP3TSDR DNA methylation analysis

Genomic DNA was extracted using DNeasy Blood & Tissue kit (Qiagen) and bisulfite was converted using EpiTect Bisulfite Kit (Qiagen). High resolution melt analysis was performed according to the following steps: forward primer—TTGGGTAAAGTTTGTAGGATAG, reverse primer—ATCTAAACCCTATTATACAACCCC, and Precision Melt Supermix (BioRad) were used for PCR. Amplification and detection of DNA were performed with the CFX96 Touch Real-Time PCR Detection System (BioRad). EpiTect Control DNA (Qiagen) was used for generating standard curves. The reaction conditions for DNA amplification were 95 °C for 2 minutes, 44 cycles of 95 °C for 15 seconds, 60 °C for 30 seconds, and 72 °C for 30 seconds, followed by 95 °C for 30 seconds and 60 °C for 1 minute. Melting was performed from 71 °C to 86 °C with 0.1 °C increment at a melt rate of 10 seconds/step. DNA methylation analysis was performed using CFX Maestro Software (BioRad).

## 2.9. Activation assay

Rested Tregs were washed and resuspended in X-VIVO 15 media, followed by overnight stimulation with anti-CD3/CD28 beads, or IL23R-coated beads (1-2 Treg:1 bead, ThermoFisher Scientific), or colon biopsy-derived cells (1 Treg:1 cell). Expression of activation marker CD69 was assessed by flow cytometry and reported as percentage or fold change between biopsy-induced activation and basal activation.

## 2.10. Suppression assay of T-cell proliferation

Rested Tregs were left untreated or activated with anti-CD3/CD28 beads or IL23R-coated beads. In parallel, allogeneic CD4<sup>+</sup> responder T cells (Tconv) were labeled with cell proliferation dye eF450 (ThermoFisher Scientific) and stimulated with anti-CD3/CD28 beads (3 Tconv:1 bead, ThermoFisher Scientific). After overnight stimulation, beads were removed from Tconv prior to coculture or transwell culture with Tregs. After 3 days, the proliferation of Tconv was determined by measuring the fluorescence of eF450 by flow cytometry. % Suppression of Tconv proliferation was calculated using the following formula:

$$100\% - \frac{\% \text{ of Tconv proliferation in the presence of Treg}}{\% \text{ of Tconv proliferation (Tconv cultured alone)}}$$

## 2.11. Monocyte isolation and culture

Monocytes were isolated from PBMCs using Classical Monocyte Isolation Kit (Miltenyi Biotec) according to the manufacturer's instructions. Monocytes were differentiated for 6 days in X-VIVO 15 media (Lonza) supplemented with 100 ng/mL GM-CSF and 50 ng/mL IL-4 (Miltenyi Biotec) to generate immature monocyte-derived dendritic cells (imDCs), followed by 24 hours treatment with 100 ng/mL LPS (Sigma) to generate mature DC (mDC).

## 2.12. DC suppression assay and MLR

IL23R-CAR Tregs were treated with or without anti-CD3/CD28 beads or IL23R-coated beads prior to coculture with

imDC or mDC. After 3-day coculture, Tregs were labeled with anti-CD2 and CD3 microbeads and depleted using magnetic columns (Miltenyi Biotec). DC phenotype was analyzed by their surface expression of costimulatory molecules CD80, CD86, and CD40 and antigen presentation molecule HLA-DR using flow cytometry. The capacity of DC to induce proliferation of naïve T cells was measured in MLR. Specifically, allogeneic naïve CD4 T cells were isolated from PBMCs using naïve CD4<sup>+</sup> T Cell Isolation Kit II (Miltenyi Biotec) and labeled with cell proliferation dye eF450 (ThermoFisher Scientific). After 3-day coculture with Tregs, DCs were enriched and cocultured with 25 000 naïve CD4 T cells at various ratios. After 6 days, the number of T cells was determined by flow cytometry.

## 2.13. Xenograft tumor model for human IL23R-CAR Treg distribution study

NOD-Prkdc<sup>scid</sup>-IL2rg<sup>Tm1/Rj</sup> (NXG) were obtained from Janvier Labs (Le Genest-Saint-Isle, France). Eight-week-old mice were housed in containment isolators and habituated for 1 week prior to experimental use. To facilitate noninvasive detection of human CAR Tregs *in vivo*, Tregs were transduced to expressed firefly luciferase and monitored by bioluminescence imaging. Five million wild-type or IL23R<sup>hi</sup>-Jurkat cells in 100 µl of BD Matrigel (Sigma-Aldrich) were injected subcutaneously into 2 flank regions of NXG mice. Twenty-one days after tumor cell inoculation, one million IL23R-CAR<sup>+</sup>, IL23R-ΔCAR<sup>+</sup>, or ΔNGFR<sup>+</sup> Luc Tregs were administered intravenously with 100 µL of Proleukin S (25 × 10<sup>3</sup> IU)/IL2 Ab (0.35 µM) complex (Clinigen, BD Biosciences). Mice were randomly assigned to groups based on tumor volumes before Treg injection. Tumor volumes (V) were estimated twice per week from caliper measurements of length (L) and width (W) and calculated as V = (W<sup>2</sup> × L)/2. Assessment of Luc-Treg cell trafficking was performed using bioluminescence (BLI). Animals were injected with an intraperitoneal dose of 100 mg/kg D-luciferin (Promega) and after 5 minutes, imaged with the IVIS Lumina S5 imaging system (Perkin Elmer). BLI data were analyzed using Living Image software (Perkin Elmer). BLI signal is reported as total flux in each tumor (photons/second).

## 2.14. Immunohistochemistry

Hematoxylin and eosin (H&E) staining was performed on formalin-fixed paraffin-embedded colon or ileum sections for pathology analysis. The sections with moderate-severe CD features were incubated with anti-IL23R or isotype antibodies (mouse IgG2b, R&D Systems) followed by visualization with Envision Flex HRP (Agilent). Negative controls were performed by omitting the primary antibody, and nuclei were stained with Mayer's Hematoxylin. Sections were coverslipped with DePex. The immunostained sections were analyzed by a histopathologist. In all cases, a comparison of IL23R antibody binding with nonimmune mouse IgG2b and antibody diluent alone (no primary) was made to interpret specific IL23R antibody immunoreactivity. The immunostaining was scored from 1+ (weak staining) to 3+ (strong staining), and the isotype control staining was subtracted from the IL23R antibody staining to access the specific IL23R staining. For samples with heterogeneous staining, the combined score was applied as previously described.<sup>50,51</sup> Briefly, each intensity of staining was scored independently and then multiplied

by the score percentage. The summed results of all intensity of staining were shown as combined score. Immunostaining intensity is rated as follows: 0, none; 1, weak; 2, moderate; 3, intense. The percentage of positive cells is graded as follows: 0, none; 1, 1%-25%; 2, 26%-50%; 3, 51%-75%; 4, 76%-100%.

### 2.15. Proximity extension assay

Plasma proteins were analyzed using Olink Target 96 Immune Response and Inflammation panels (184 proteins) and reported as normalized protein expression on a  $\log_2$  scale (NPX). Correlation analysis between protein NPX values and CD69-fold change was performed using `cor()` function implemented in R with `method="spearman"`.

### 2.16. mRNA-seq and analysis

Libraries for RNA-seq were generated using TruSeq Stranded mRNA kit (Illumina). Libraries were validated on the Fragment Analyzer platform (AATI) and concentrations were determined using the Qubit fluorometer (ThermoFisher Scientific). Sequencing was performed using a S4 flow cell on an Illumina NovaSeq 6000. Sequence reads were trimmed to remove possible adapter sequences and nucleotides with poor quality using Trimmomatic<sup>52</sup> v.0.36. The trimmed reads were mapped to the Homo sapiens GRCh38 reference genome available on ENSEMBL using the STAR aligner<sup>53</sup> v.2.5.2b. Unique gene hit counts were calculated by using featureCounts<sup>54</sup> from the Subread package v.1.5.2. Gene expression counts were then normalized and variance stabilized using DESeq2.<sup>55</sup> Weighted Gene Coexpression Network Analysis (WGCNA, v1.72)<sup>56</sup> was performed on the variance stabilized gene expression matrix using the top 10 000 highly variable genes with the following parameters: `soft power=10`, `deepSplit=4`, `minClusterSize=30`, `method="hybrid"`. Correlation analysis between CD69-fold change and either gene expression or WGCNA module expression was performed using `cor()` function implemented in R with `method="spearman"`. Enrichment analysis of genes from positively correlated WGCNA modules was performed using `enrichR`<sup>57</sup> R package v3.2.

### 2.17. Statistics

All data were analyzed with one-way or 2-way ANOVA with Dunnett's or Tukey's or Sidak's multiple comparisons using GraphPad Prism 9 (GraphPad Software Inc.). Data were considered significant at a *P* value of less than 0.05. All data are reported as the arithmetic or geometric mean  $\pm$  SEM or median as appropriate.

### 2.18. Study approval

All subjects enrolled in the SG450-001 phase 0 study provided informed written consent for blood or tissue donation according to protocols approved by the independent ethics committee and French National Agency for the Safety of Medicines and Health Products (ANSM). Intestinal biopsy tissues were collected from the most affected or the least affected areas of the colon and/or terminal ileum during the colonoscopy procedure. A whole blood sample was also collected at the colonoscopy visit.

All animal experiments were performed in an accredited mouse facility in accordance with the guidelines of the French Veterinary Department. The animal protocols were approved by the French animal ethics committee.

## 3. Results

### 3.1. IL23R expression is upregulated in the gut of CD patients

To confirm the presence of the target antigen IL23R in CD patients, immunohistochemical analysis was performed in biopsies from CD and healthy subjects. An increase in IL23R staining was observed in the biopsies from active CD subjects compared to healthy donors (HDs; Figure 1A). Due to heterogeneous staining presented in multiple biopsies from the same donor, a combined score was applied as previously described<sup>50,51</sup>: the median combined score was 7 for CD subjects compared to 1 for HDs (Figure 1B). Interestingly, mild nonspecific chronic inflammation was identified by H&E pathology review (data not shown) in one healthy subject with higher IL23R expression (combined score = 3). In moderate-severe CD subjects, specific IL23R immunoreactivity was seen in the mononuclear cells in the lamina propria in colon or ileum biopsies (Figure 1C). In the 14 biopsies analyzed, 13 out of 14 samples showed IL23R expression in the lamina propria (median score = 2, median percentage = 10%) (Figure 1D). Consistent with protein expression, we also measured an increase in IL23R mRNA in biopsy compared to PBMC from CD subjects (Supplementary Figure S5A). Overall, expression of the target antigen IL23R is upregulated in the mucosa of CD subjects.

To assess the off-target effect of IL23R-CAR in other tissues, we performed tissue cross-reactivity analysis using human normal tissue sections and tissue microarrays from 45 tissue types (Supplementary Table S1) from 3 HDs (Supplementary Figure S1A). Tissue sections were stained with IL23R-scFv-multimer-derived antibody to verify the target specificity of IL23R-CAR. A distinct sporadic staining was only observed in gut tissue (e.g. colon and ileum), while some weak reactivity could be observed in the dorsal/ventral horn of the spinal cord (1 out of 3 donors). All other tissues remained free of signal.

### 3.2. Human IL23R-CAR Tregs display negligible tonic signaling and maintain regulatory phenotype following expansion and chronic antigen stimulation

To engineer an anti-IL23R CAR, we screened a library of fully human anti-IL23R scFvs and cloned the optimal candidate into a lentiviral vector to generate an IL23R-CAR. The CAR contained anti-IL23R scFV, a hinge domain, a transmembrane domain, and a CD28-CD3 $\zeta$  signaling domain. IL23R- $\Delta$ CAR, an IL23R-CAR lacking the signaling domain, was constructed as a nonfunctional negative control (Figure 2A). To generate human IL23R-CAR Tregs, CD4<sup>+</sup>CD25<sup>+</sup>CD127<sup>lo</sup>CD45RA<sup>+</sup> naive Tregs were sorted from the peripheral blood of HDs and expanded prior to lentiviral transduction with a CAR construct. IL23R-CAR Tregs were analyzed after restimulation with anti-CD3/CD28 beads. CAR expression monitoring showed that transduction efficiencies ranged from 40% to 65% (Figure 2B). IL23R-CAR Tregs displayed negligible tonic signaling with basal activation level (% CD69) similar to the control  $\Delta$ CAR-Tregs or untransduced (UT) Tregs (Figure 2C). IL23R-coated beads were used to assess CAR-specific activation of IL23R-CAR Tregs. Following overnight exposure to IL23R-coated beads, IL23R-CAR Tregs significantly upregulated CD69 to a level comparable to TCR stimulation using anti-CD3/CD28 beads (Figure 2C); this was not observed in untransduced

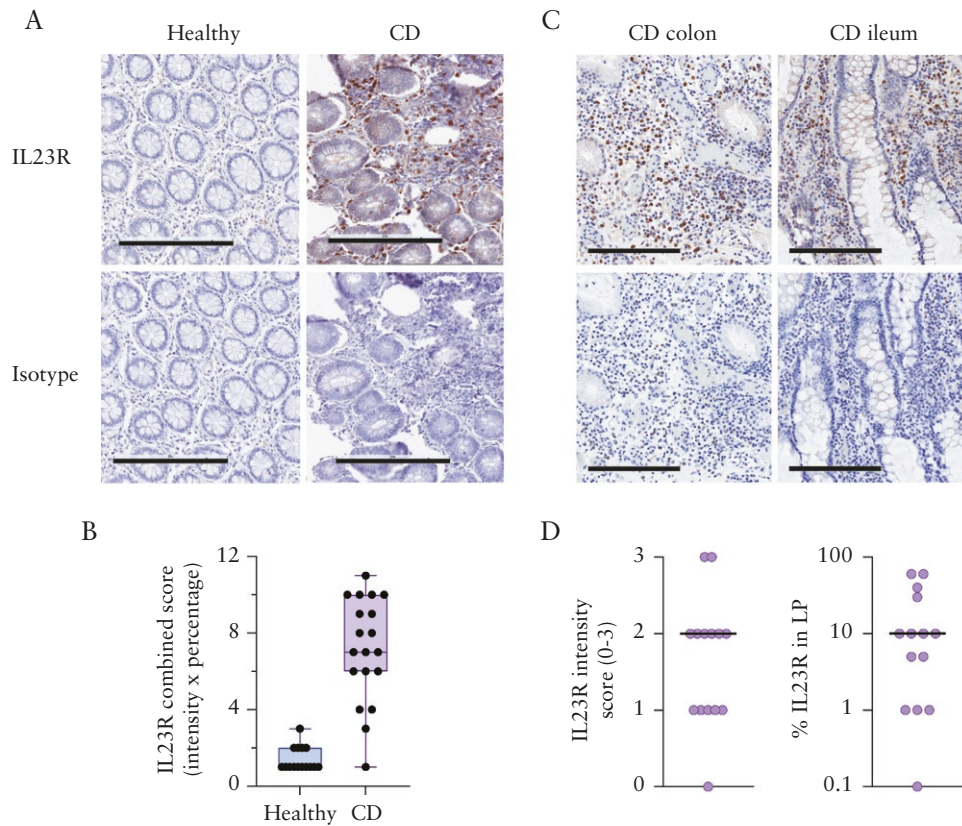


**Figure 1** IL23R expression in intestinal biopsies from CD patients. (A) Representative human IL23R or isotype (mouse IgG2b) staining and (B) combined score (intensity score × percentage score) of IL23R in the colon lamina propria of healthy or CD subjects. The IL23R score reflects the percentage of IL23R positive cells graded as follows: 0, none; 1, 1%-25%; 2, 26%-50%; 3, 51%-75%; 4, 76%-100%. The IL23R intensity score is determined by immunostaining intensity rated as follows: 0, none; 1, weak; 2, moderate; 3, intense. Scale bar is 200  $\mu$ m. (C) IL23R or isotype staining of representative colon or ileum section from 2 CD subjects. (D) IL23R intensity score and percentage of IL23R<sup>+</sup> cells in lamina propria. Pool of 14 samples from 10 moderate-severe CD subjects.

or non-signaling IL23R- $\Delta$ CAR Tregs. IL23R-CAR Tregs also upregulated other activation-associated markers, GARP and 4-1BB, following CAR stimulation (Supplementary Figure S2). IL23R-CAR Tregs maintained regulatory T-cell phenotype following expansion, with high expression of CD4, CD25, CD45RA, CTLA-4, FOXP3, HELIOS, and FOXP3 TSDR demethylation (Figure 2D, E).

To mimic the CD microenvironment, we established an *in vitro* model and chronically challenged CAR Tregs with their target antigen (Figure 2F). Consistent with the findings of Canavan et al.,<sup>19</sup> no gain of inflammatory cytokine IL-17A was measured after chronic stimulation on day 26 (Figure 2G), suggesting IL23R-CAR Tregs are resistant to Th17 conversion. To further challenge IL23R-CAR Tregs in a proinflammatory condition, we stimulated the cells with TNF $\alpha$ , IL-1 $\beta$ , and IL-6 every 2 days. After 12 days of chronic stimulation (days 15-26), IL23R-CAR Tregs continued to express high levels of FOXP3 in a proinflammatory cytokine environment (Figure 2H). Together, IL23R-CAR expression did not alter the phenotype of human Tregs following expansion or chronic antigen stimulation, fulfilling the basic requirement of a cell therapy product.

### 3.3. IL23R-CAR Tregs mediate target antigen-specific immunosuppression and immunomodulation

To evaluate the function of IL23R-CAR Tregs, their ability to inhibit the proliferation of CD4 responder T cells (Tconv) was examined in a suppression assay. IL23R-CAR Tregs and

control Tregs were left untreated (NS) or were stimulated through their CAR or TCR prior to coculture or transwell culture with Tconv. Compared to NS, IL23R-CAR Tregs significantly inhibited the proliferation of Tconv upon prestimulation with either IL23R-coated beads or anti-CD3/CD28 beads, demonstrating an antigen-specific immunosuppression (Figure 3A). In contrast, control Tregs were only able to suppress Tconv proliferation when stimulated via their TCR (Figure 3A). When cultured with Tconv in a transwell system to assess their contact-independent suppressive activities, IL23R-CAR Tregs also induced a significant, but less pronounced inhibition of Tconv proliferation (Figure 3A). In addition to IL23R-coated beads, Jurkat cells expressing high or low levels of IL23R, named IL23R<sup>hi</sup>-Jurkat and IL23R<sup>lo</sup>-Jurkat, respectively (Supplementary Figure S3A, B), can also engage IL23R-CAR and elicit IL23R-dependent activation and inhibition of Tconv proliferation *in vitro* (Supplementary Figure S3C, D).

Given that CAR Tregs-mediated DC suppression *in vitro* appears to be a superior predictor of *in vivo* Treg function,<sup>58</sup> the ability of Tregs to suppress APCs has been suggested as an important functional criterion for an effective CAR-Treg therapeutic product.<sup>59</sup> Hence, we tested whether IL23R-CAR Treg inhibited DC maturation and function *in vitro*. Both CD127<sup>low</sup> Tregs (CD4<sup>+</sup>CD127<sup>low</sup>CD25<sup>+</sup>, Supplementary Figure S4) and naïve Tregs (CD4<sup>+</sup>CD127<sup>low</sup>CD25<sup>+</sup>CD45RA<sup>+</sup>, Figure 3B, C) have been tested and showed similar results. Monocyte-derived imDC and mDC were cocultured with untreated or polyclonally activated, or CAR antigen-stimulated

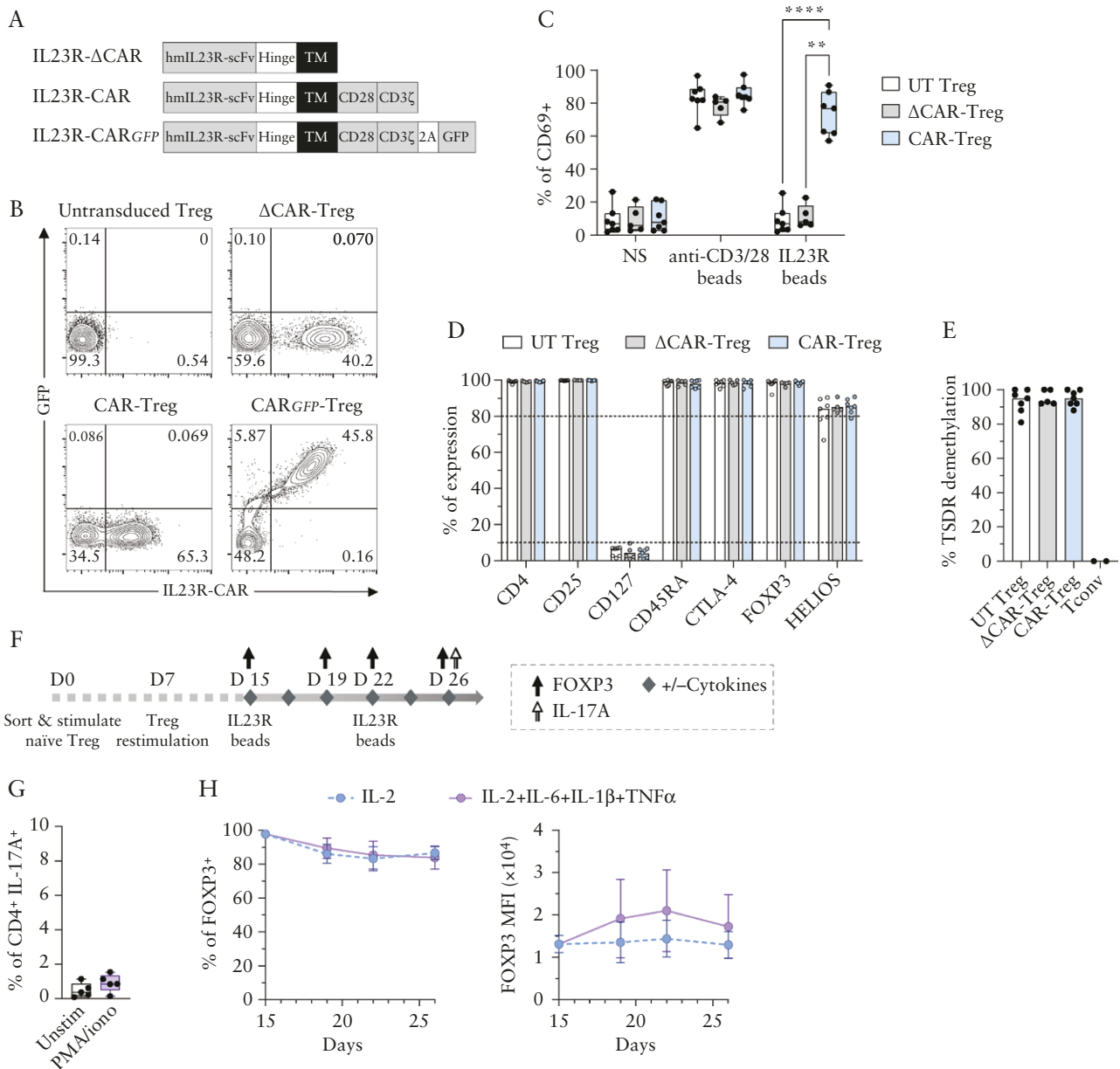


**Figure 2** IL23R-CAR Tregs maintain regulatory phenotype during expansion and after antigen stimulation. (A) Schematic diagram of the IL23R-CAR and the control IL23R- $\Delta$ CAR which lacks a signaling domain. (B) Naive Tregs were left UT or transduced with a nonsignaling truncated IL23R-CAR (IL23R- $\Delta$ CAR), IL23R-CAR, or GFP-tagged IL23R-CAR (IL23R-CAR<sup>GFP</sup>). After 12 days of expansion, cells were analyzed for CAR expression. (C) Percentage of CD69 expression on UT Tregs or CAR Tregs after overnight activation with culture media (NS), anti-CD3/CD28 beads, or IL23R coated beads. Two-way ANOVA with Tukey's multiple comparisons test was performed. (D) Phenotype and (E) TSDR demethylation of IL23R-CAR Tregs after 12 days of expansion. (F) Schematic diagram of IL23R-CAR Treg chronic stimulation with IL23R-coated beads at days 15 and 22 in the presence of IL-2 alone or IL-2 combined with proinflammatory cytokines (IL-6, IL-1 $\beta$ , and TNF $\alpha$ ) replenished every 2 days. (G) Percentage of intracellular IL-17A produced by IL23R-CAR Tregs at day 26. (H) Percentage and intensity of FOXP3 expression in IL23R-CAR Tregs after chronic stimulation in the presence of proinflammatory cytokines. Abbreviations: PMA/iono, stimulated with PMA and ionomycin; Unstim, not treated; UT, untransduced.

IL23R-CAR Tregs. Mature DC showed a higher surface expression of costimulatory molecules CD80, CD86, and CD40 and antigen presentation molecule HLA-DR compared to imDC (Supplementary Figure S4A). Consistent with previous studies,<sup>60,61</sup> Treg-treated DC displayed a less mature phenotype with decreased cell surface expression of these markers (Figure 3B; Supplementary Figure S4A). Importantly, stimulating IL23R-CAR Tregs through their TCR or CAR further inhibited DC maturation (Figure 3B, C; Supplementary S4A). In accordance with their partial mature phenotype, IL23R-CAR Treg-treated mDC showed decreased capacity to induce allogeneic

CD4 T-cell proliferation in a mixed leukocyte reaction (MLR; Supplementary Figure S4B). Overall, these results demonstrate that the expression of IL23R-CAR on human Tregs significantly augments their ability to suppress both T cells and antigen-presenting cells in the presence of IL23R.

### 3.4. Human IL23R-CAR Tregs migrate to IL23R-expressing tissue *in vivo*

To evaluate whether anti-IL23R CAR expression on Tregs can promote their migration to an IL23R-expressing tissue *in vivo*, we developed a xenograft mouse model in which wild-type

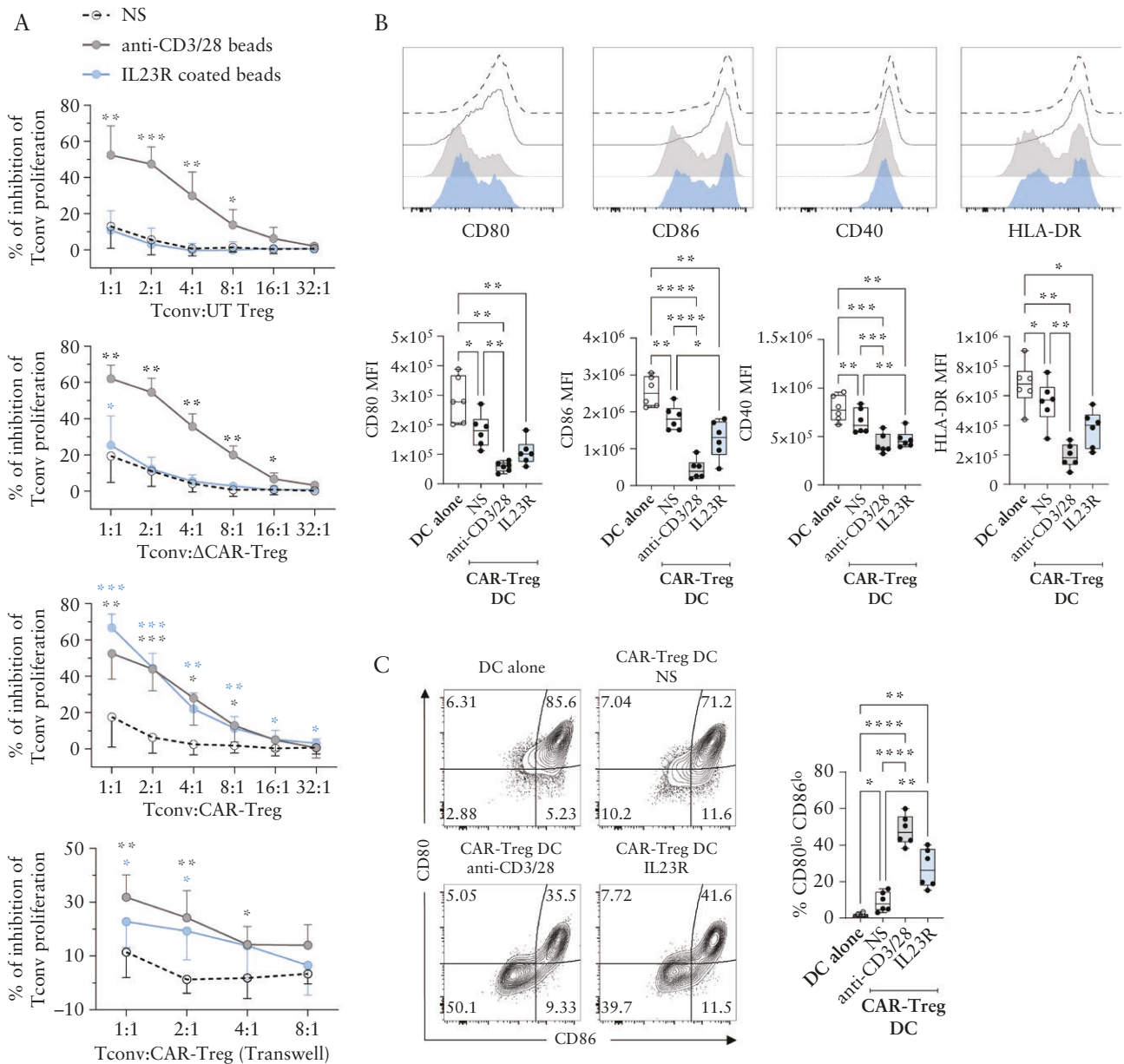


**Figure 3** IL23R-CAR Tregs exhibit IL23R-dependent suppressive activity *in vitro*. (A) Suppression of polyclonally stimulated responder T-cell (Tconv) proliferation by untransduced (UT) Tregs, IL23R-ΔCAR-Tregs, or IL23R-CAR Tregs in coculture or transwell culture. Tregs were prestimulated with culture media (NS), anti-CD3/CD28 beads, or IL23R-coated beads. Data are shown as mean ± SD ( $n = 7$ ). Two-way ANOVA with Dunnett's multiple comparisons test was performed. \* $p < 0.05$ , \*\* $p < 0.01$ , \*\*\* $p < 0.001$ . (B, C) IL23R-CAR Tregs inhibit the maturation of monocyte-derived dendritic cells (DC). Autologous immature DCs were treated with LPS to induce maturation (DC alone) or cocultured with prestimulated IL-23R-CAR Tregs in the presence of LPS (CAR-Treg DC). After 3-day coculture, DC phenotype was analyzed by (B) surface expression of CD80, CD86, CD40, and HLA-DR, (C) percentage of immature DC. One-way ANOVA with Tukey's multiple comparisons test was performed. \* $p < 0.05$ , \*\* $p < 0.01$ , \*\*\* $p < 0.001$ , \*\*\*\* $p < 0.0001$ .

and IL23R<sup>hi</sup>-Jurkat cell lines (Supplementary Figure S3, shown as IL23R<sup>-</sup> or IL23R<sup>+</sup> tumors in Figure 4) were injected subcutaneously into 2 separate flank regions. Also, IL23R<sup>-</sup> and IL23R<sup>+</sup> tumors were engrafted in 2 orientations to minimize the effects of location on tumor growth (Figure 4B). Three weeks after tumor engraftment, luciferase-expressing ΔNGFR-Luc Tregs, IL23R-ΔCAR-Luc Tregs, or IL23R-CAR-Luc Tregs were injected intravenously, and their migration was monitored using bioluminescence imaging (Figure 4A, B). Six days post-Treg injection, scarcely any control Tregs (ΔNGFR-Luc or IL23R-ΔCAR-Luc Tregs) were seen in the tumor site, as shown with almost undetectable luciferase activity. On the contrary, IL23R-CAR-Luc Tregs accumulated specifically in the IL23R<sup>+</sup>

but not the IL23R<sup>-</sup> tumors as shown in imaging (Figure 4B) and the quantification of the bioluminescence signals (Figure 4C). The increase in bioluminescence was not the consequence of variability in tumor proliferation as all the tumors were of similar size (Figure 4D). These results demonstrate that IL23R-CAR Tregs have the capacity to migrate and remain in tissues where their target antigen IL23R is expressed.

### 3.5. Activation of human IL23R-CAR Tregs by intestinal cells from CD patients is associated with transcriptomic and proteomic patterns

To determine whether IL23R-CAR Tregs can recognize IL23R-expressing cells in CD patients, we stimulated allo

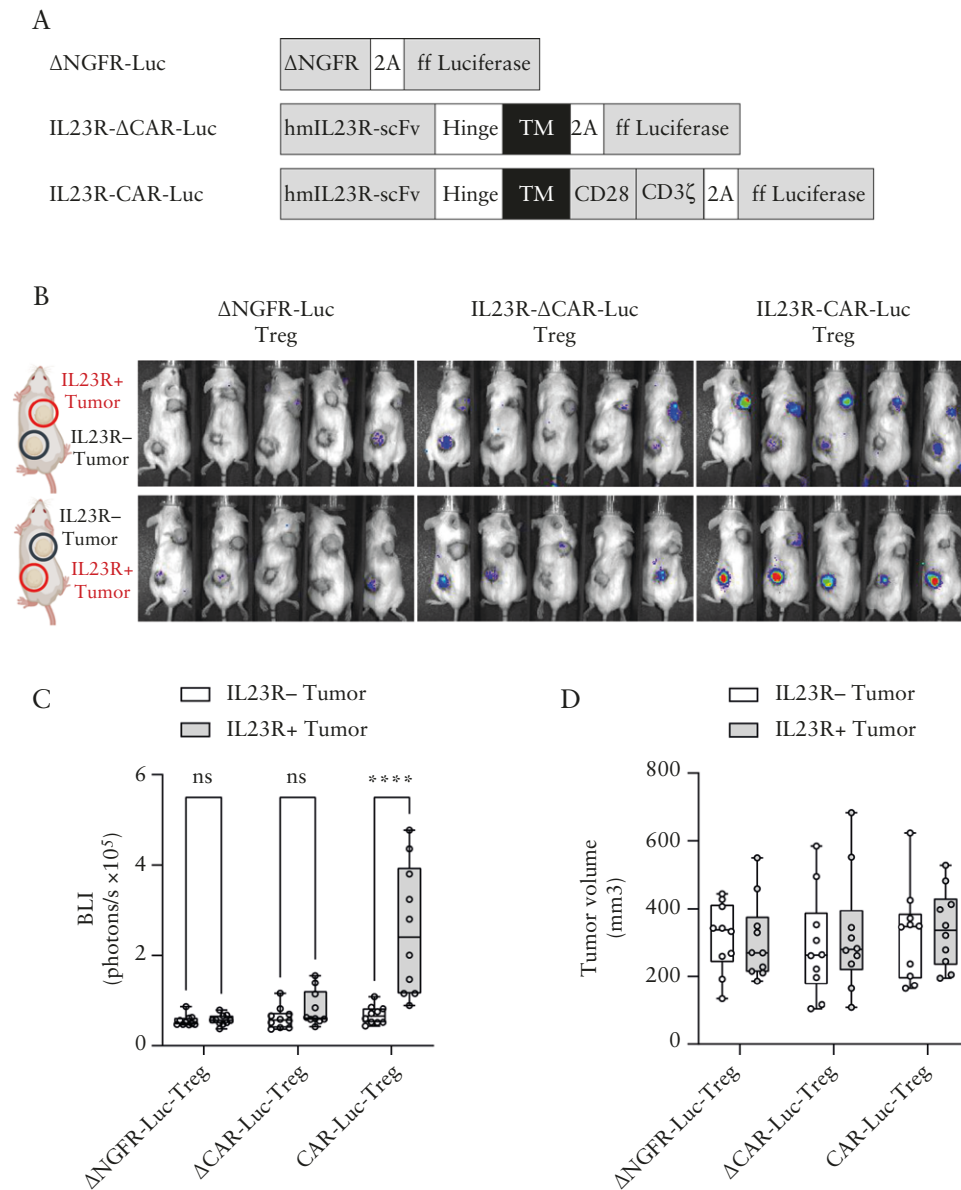


**Figure 4** IL23R-CAR Tregs migrate into human IL23R-expressing tissues. (A) Schematic diagram of the luciferase-expressing lentiviral constructs. (B) Three weeks after engraftment of IL23R<sup>-</sup> and IL23R<sup>+</sup> tumors in both orientations, luciferase-expressing human ΔNGFR-Tregs, IL23R-ΔCAR Tregs, or IL23R-CAR Tregs were injected intravenously. After 6 days, luciferase expression was monitored in mice by quantification of the total bioluminescence signal (photons/sec) in IL23R<sup>-</sup> or IL23R<sup>+</sup> tumors. (C) Data are presented as box and whisker plots. Each dot represents an individual tumor ( $n = 10$  per group, 2-way ANOVA with Sidak's multiple comparisons test, \*\*\*\* $p < 0.0001$ ; ns, not significant). (D) As a control, the size of the tumors was measured in all the conditions (no statistical differences).

IL23R-CAR Tregs with cells isolated from CD patient colon biopsies in an activation assay. CD4<sup>+</sup>CD127<sup>low</sup>CD25<sup>+</sup> Tregs (CD127<sup>low</sup> Tregs) isolated from HDs were transduced with IL23R-CAR<sub>GFP</sub> or control IL23R-ΔCAR<sub>GFP</sub> and expanded prior to overnight culture with cell suspensions from colon biopsies (Figure 5A). In parallel, CAR Tregs were left untreated or stimulated with anti-CD3/CD28 beads or IL23R-coated beads. Similar to naïve IL23R-CAR Treg (Figure 2C), CD127<sup>low</sup> IL23R-CAR Tregs significantly upregulated activation marker CD69 in response to IL23R beads or anti-CD3/CD28 stimulation (Figure 5B). Importantly, IL23R-CAR Tregs but not control IL23R-ΔCAR Tregs responded to cells from severe CD colon biopsies with a significant upregulation of CD69, suggesting the presence of IL23R in biopsy samples was sufficient to engage and activate IL23R-CAR (Figure

5C, left; Supplementary Table S2). Although not statistically significant, a slight increase of CD69 was also observed in coculture with more inflamed colon biopsies from mild-moderate CD subjects (Figure 5D; Supplementary Table S2). Moreover, the upregulation of CD69 was more pronounced in response to biopsies with higher levels of inflammation, i.e. higher levels of infiltrating inflammatory cells (Figure 5C, left, shown as biopsy more inflamed). Similar results were observed with activation marker GARP (glycoprotein-A repetitions predominant, Figure 5C, right).

To understand the molecular basis of IL23R-CAR Treg activity towards their target from CD patients, we performed transcriptomic profiling (RNA-Seq) of CD colon biopsy samples ( $N = 17$ , more inflamed areas;  $N = 20$ , less inflamed areas) and plasma protein profiling ( $N = 11$ ). The CD69-fold

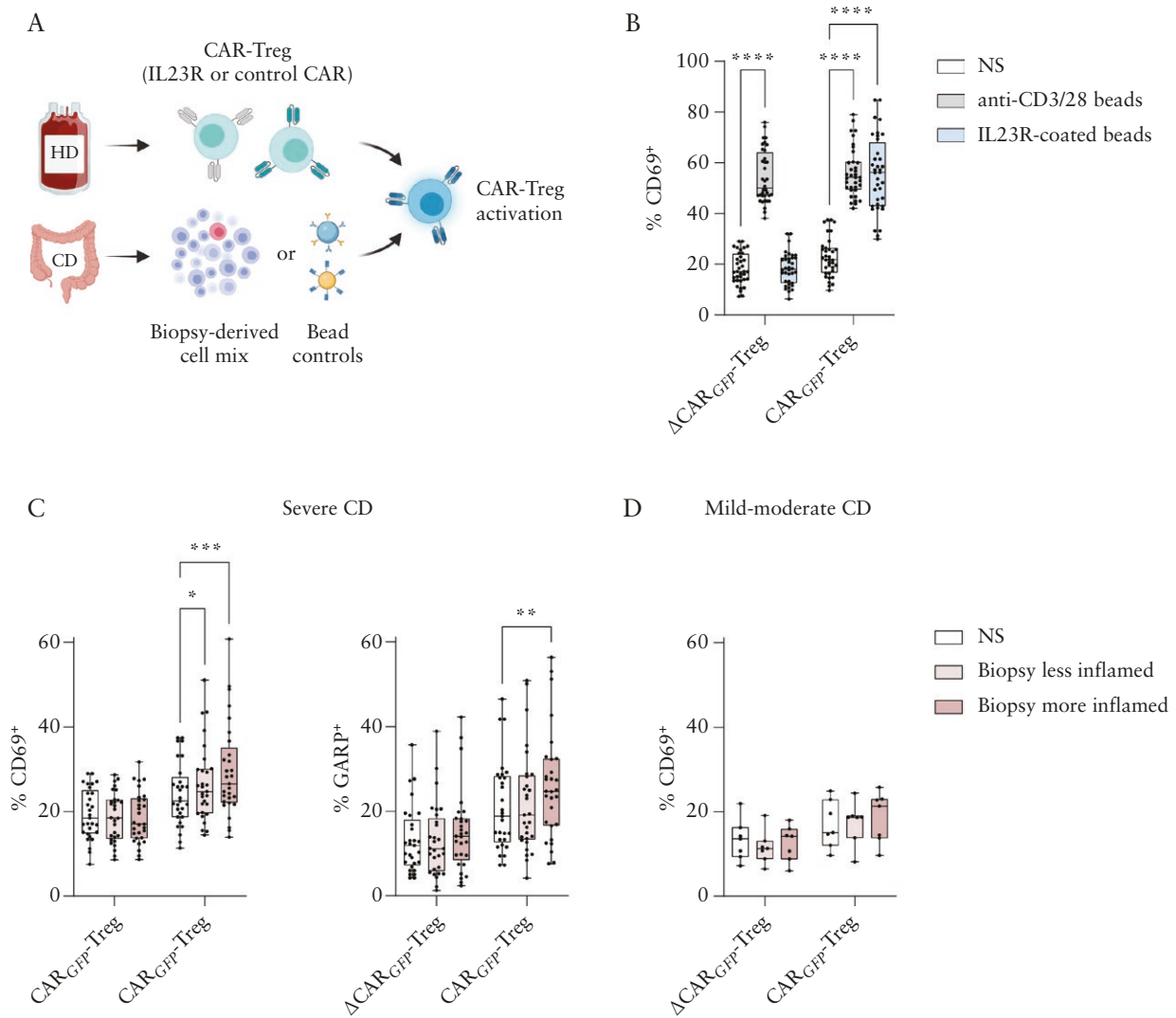


**Figure 5** Colon biopsy-derived cells from CD patients induce IL23R-CAR Treg activation. (A) Schematic diagram of activation assay. Created with BioRender.com. (B) Percentage of CD69 expressing IL23R- $\Delta$ CAR<sub>GFP</sub> or IL23R-CAR<sub>GFP</sub> Tregs after overnight stimulation with culture media (NS), anti-CD3/CD28 beads, or IL23R-coated beads. (C, D) Percentage of activated (CD69 or GARP expressing) IL23R- $\Delta$ CAR<sub>GFP</sub> or IL23R-CAR<sub>GFP</sub> Tregs after overnight stimulation with culture media (NS) or colon biopsy-derived cells from (C) severe or (D) mild-moderate CD patients. Biopsies from less or more inflamed areas were collected from the same patients. Two-way ANOVA with Dunnett's multiple comparisons test was performed.

change between biopsy-induced activation and basal activation (NS) of IL23R-CAR Tregs was used as a surrogate outcome variable in the correlation analysis. To capture the heterogeneity and to further reduce the dimensionality of the RNA-seq data, we performed weighted genes coexpression network analysis (WGCNA) on normalized RNA-seq data and identified 5 WGCNA modules that are positively correlated ( $N = 13$ , Spearman  $\rho > 0.7$  and FDR- $p < 0.05$ ) with CD69-fold change. The genes from those 5 modules combined are enriched with pathways/processes related to inflammation and immune regulation (Figure 6A). Through quantification of plasma proteins with ELISA, we have found a strong correlation between plasma IL-23 and CD69-fold change (Figure 6B). To measure the extent of microbial translocation and intestinal inflammation, plasma 16S rDNA and calprotectin were quantified. Despite their upregulation in CD or severe CD (Supplementary Figure S5B, C; Supplementary Table S3), we did not observe an association with CD69-fold change. Moreover, plasma protein screening using proximity

extension assay revealed additional proteins associated with CD69-fold change, including CCL20, CXCL1, CXCL6, and CXCL10 (Figure 6C).

#### 4. Discussion

A CAR-Treg therapy that redirects Tregs to target specific tissues, resulting in long-lasting immune tolerance, could represent a major breakthrough in the treatment of autoimmune and chronic inflammatory diseases. Here, we describe the development of IL23R-CAR Treg therapy and explore its potential for the treatment of CD. Our CAR Treg platform consists of introducing a CAR into naïve CD4<sup>+</sup>CD45RA<sup>+</sup>CD127<sup>lo</sup>CD25<sup>hi</sup> Tregs, that express high level of FOXP3. The IL23R-CAR is comprised of a highly specific scFv and a CD28/CD3 $\zeta$  signaling domain that is being used in our current leading clinical trial STEADFAST.

The importance of the IL-23/IL23R pathway in the pathogenesis of IBD has been well established by human genetic

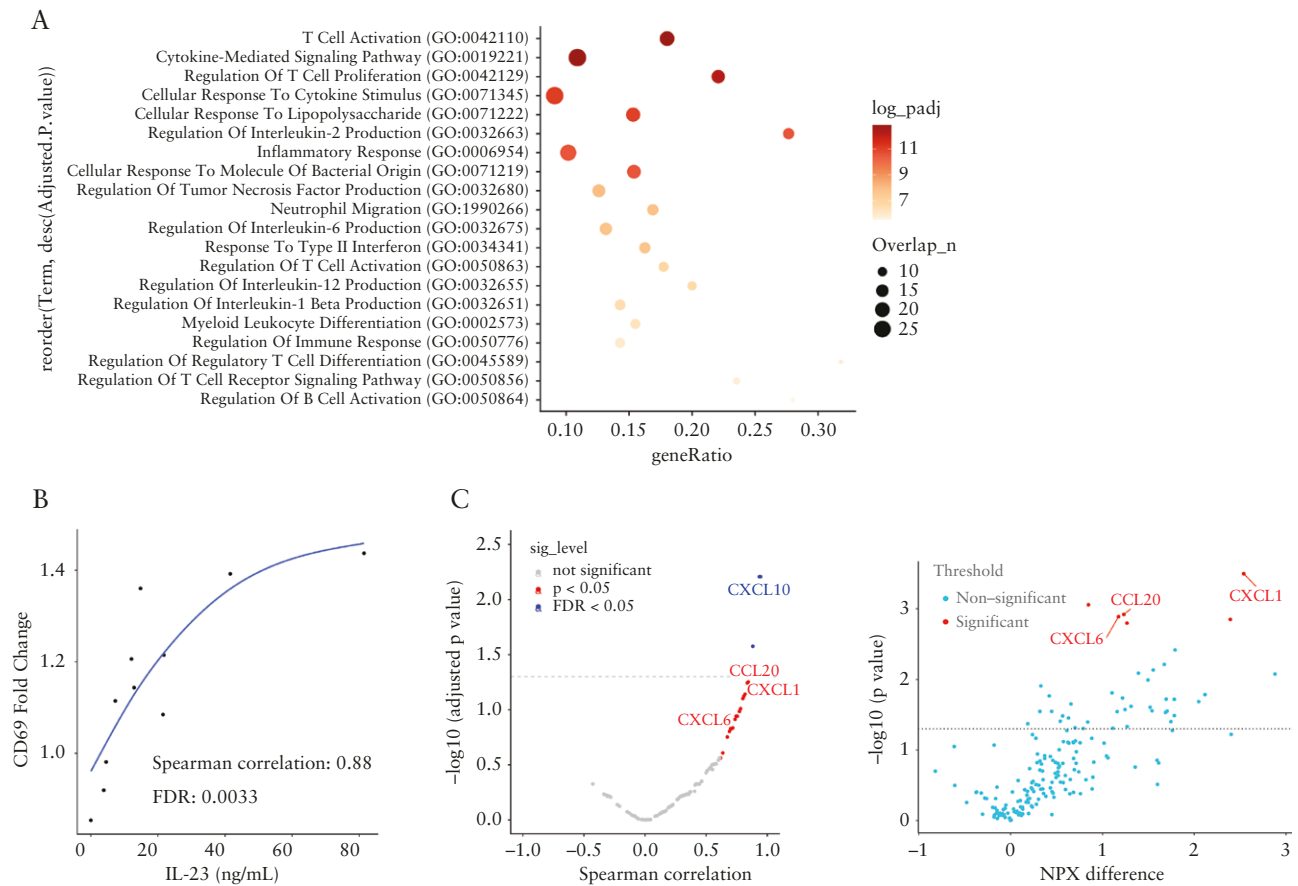


**Figure 6** Transcriptomic and proteomic patterns associated with CD biopsy-induced IL23R-specific Treg activation. (A) Transcriptomic profiling (RNA-Seq) was performed on CD colon biopsy samples. The CD69-fold change between biopsy-induced activation and basal activation (NS) of IL23R-CAR Tregs was used as a surrogate outcome variable in the correlation analysis. (A) Correlation analysis between WGCNA modules and biopsy-induced IL23R-specific CAR activation was performed ( $N = 11$ ). Enrichment analysis of genes within positively correlated modules was performed using EnrichR. Top 20 ranked Gene Ontology (GO) terms according to adjusted  $p$  value are displayed here. Log<sub>padj</sub>, log<sub>10</sub> of the adjusted  $p$  value; Overlap<sub>n</sub>, number of enriched genes in a GO term; gene ratio, percentage of enriched genes in the given GO term. (B) Correlation analysis between plasma IL-23 concentration and biopsy-induced IL23R-specific CAR activation ( $N = 11$ ). A line is used to approximate the relationship between the 2 variables. (C) Plasma protein screening using proximity extension assay. Left, correlation analysis between normalized protein expressions (NPX) and patient biopsy-induced IL23R-specific CAR activation ( $N = 11$ ). The dotted line represents the FDR threshold of 0.05. Right, volcano plot of the Group strong ( $N = 4$ ) versus Group weak/no ( $N = 7$ ) IL23R-specific CAR activation. The dotted line represents the uncorrected significance threshold of 0.05. The x-axis depicts the NPX difference between the groups for each protein measured.

association and the efficacy of IL-23 blockers.<sup>43,44,49</sup> IL23R is expressed in various immune cell populations, including conventional T cells, innate T cells, innate lymphoid cells (ILC), B cells, and myeloid cells.<sup>62</sup> However, the surface expression of IL23R and its induction are still poorly characterized partly due to the lack of a reliable anti-IL23R antibody for flow cytometry analysis. In the FLAG-tagged IL23R<sup>low</sup> Jurkat cell line, we observed a FLAG<sup>+</sup> population was not labeled with anti-IL23R antibody, suggesting that anti-IL23R antibody failed to recognize all the IL23R<sup>+</sup> cells (Supplementary Figure S3B). In CD biopsies, we could identify multiple immune cell types, particularly those that have been reported expressing IL23R, including conventional T cells, innate T cells, innate lymphocytes, etc. However, due to the lack of a reliable anti-IL23R antibody for flow cytometry, we were not able to obtain convincing data on surface IL23R staining, therefore we were not able to investigate the specific immune cell types with increased IL23R expression. Thus, we used immunohistochemistry method to examine the IL23R expression in CD patients. IL23R expression was detected on mononuclear cells within the lamina propria of active CD patients

and was upregulated in comparison with HDs. These results are in accordance with previous studies for CD and gastrointestinal (GI) GVHD.<sup>63,64</sup> In the GI-GVHD study, sequential immunostaining confirmed the enrichment of RAR $\alpha^{\text{hi}}$  T-bet<sup>+</sup> CD8 effector cells co-expressed IL23R and were expanded in IL-23-rich human GI-GVHD tissue.<sup>64</sup> Whether this population is also enriched in CD requires further investigation. Notably, scRNA-seq analyses of CD and UC (ulcerative colitis) biopsies show that ILC, resident memory T cells (Trm), and CD8<sup>+</sup>IL17<sup>+</sup> cells are cell subsets expressing IL23R. Expansion of CD8<sup>+</sup>IL17<sup>+</sup> T cells was also suggested to contribute to T-cell pathogenicity and tissue damage in UC.<sup>65,66</sup>

Our current understanding of IL23R suggests that most immune cells need to be activated to acquire responsiveness to IL-23 and the secretion of proinflammatory cytokines,<sup>62</sup> supporting the notion that IL23R acts as a tuneable target regulated by the microenvironment. Given that constant exposure of CAR to its target might induce CAR-Treg exhaustion, a tuneable target could potentially prolong the persistence and efficacy of CAR Tregs. Here, a series of target sources was used to examine IL23R-CAR Treg function,

including IL23R-coated beads, Jurkat cell lines expressing high or low levels of IL23R, and primary cells isolated from colon biopsies. Regardless of the origin of the target antigen, IL23R-CAR Tregs showed specific activation toward IL23R. Importantly, the extent of IL23R-specific activation and suppression was associated with the expression level of IL23R, resulting in Treg effects in a target dose-dependent manner. Moreover, human IL23R-CAR Tregs also have the capacity to migrate and remain in tissues where their target antigen IL23R is expressed.

In addition to the target antigen selection, the CAR design is also critical in maintaining the phenotype and function of CAR Tregs. Due to spontaneous aggregation of the CAR receptors at the cell surface, some CARs induce tonic signals in the absence of ligand stimulation.<sup>67–70</sup> Prolonged and high levels of stimulation can lead to CAR-Treg exhaustion, epigenetic changes, and complete loss of suppression *in vivo*.<sup>70,71</sup> Therefore, the selection of the CAR with the lowest tonic signaling was the main criterion for the development of our IL23R-CAR. In this study, we show that IL23R-CAR Tregs exhibit minimal tonic signaling with a basal activation similar as control or untransduced Tregs. Consistently, IL23R-CAR Tregs maintain regulatory phenotype following the expansion process, with high expression of CD4, CD25, CD45RA, CTLA-4, FOXP3, HELIOS, and TSDR demethylation.

The plasticity of Treg lineage represents a potential safety concern associated with CAR Tregs, as the conversion of CAR Tregs into CAR-T effector cells could exacerbate autoimmunity.<sup>72</sup> A homogeneous Treg population (CD4<sup>+</sup>CD25<sup>+</sup>CD127<sup>lo</sup>CD45RA<sup>+</sup>) was reported to be phenotypic and functionally stable upon *in vitro* expansion and resistant to Th17 conversion.<sup>18,19</sup> Importantly, these cells can be home to mucosal tissue, making them the most appropriate population for CAR-Treg therapy for CD.<sup>19</sup> Thus, we decided to use CD4<sup>+</sup>CD25<sup>+</sup>CD127<sup>lo</sup>CD45RA<sup>+</sup> Tregs in the development of IL23R-CAR Tregs. Similar to what Canavan et al.<sup>19</sup> and Skartsis et al.<sup>73</sup> observed, exposure to proinflammatory cytokines did not change the lineage stability of IL23R-CAR Tregs as demonstrated by the preserved high expression of FOXP3 for up to 12 days of chronic stimulation with and without the presence of proinflammatory cytokines.

It is well established that Tregs control immune responses through diverse mechanisms, including the inhibition of effector T-cell activities and the modulation of DC maturation and function.<sup>74,75</sup> This also holds true for IL23R-CAR Tregs as shown in the *in vitro* functional assays. IL23R-CAR Tregs can suppress effector T-cell proliferation, and inhibit DC maturation and function. Their suppressive ability was further enhanced upon stimulation with target antigen IL23R. These results suggest that IL23R-CAR Tregs can mediate antigen-specific immunosuppression and promote a tolerogenic microenvironment.

To analyze the *in vivo* therapeutic potential of human IL23R-CAR Tregs, our initial efforts were focused on developing a humanized mouse model of IBD using immunodeficient NSG mice. Injection of mature human PBMCs can support the survival of Tregs as they activate due to the recognition of mouse antigens and therefore produce human IL-2 which can support Treg survival. However, in this humanized model, IL23R was only minimally induced on mouse cells but not on the human T cells that engrafted in the NSG mice, and the cytokines produced by the mouse inflammatory cells did not cross-react with the human Tregs and hence, did

not induce their migration to the site of inflammation i.e the colon. Although these caveats are not present in syngeneic colitis mouse models, other factors limit their use: (i) a specific CAR design tailored for mice, (ii) the use of surrogate mouse Tregs and (iii) these models cannot accurately recapitulate the complexities of disease presentation in humans. As a result, we were not able to investigate the curative potential of human IL23R-CAR Tregs *in vivo*. To evaluate human IL23R-CAR Tregs efficacy in a physiological context, future work will focus on developing 3D culture with CD-derived organoids together with IL23R-expressing cells from CD LP. We believe this would provide a more relevant model for assessing the efficacy of human IL23R-CAR Tregs in treating CD.

Patients with CD are a heterogeneous population with a wide range of responses to treatment. In recent years, omics biomarkers have been explored to further optimize the treatment strategies for CD therapies.<sup>1,2,76</sup> Therefore, we performed transcriptomic and proteomic profiling to further characterize CD patients and hope to identify predictors of response to IL23R-CAR Treg therapy. As the biopsy samples we collected were very limited, we did not enrich specific cell type prior to running RNA-Seq analysis. Nevertheless, enrichment analysis revealed an induction of inflammation and immune regulation gene patterns, consistent with the expression of IL23R on immune cells. We further explored inflammation and immune regulation-relevant protein biomarkers in the patients' plasma and identified multiple potential candidates, many of which were chemokines. CCL8, a major chemoattractant of neutrophils, is significantly enhanced in the lamina propria of CD patients. CCL20 and its receptor CCR6 are responsible for the chemotaxis of DC and effector/memory T and B cells. CCR6 is also essential for the recruitment of Th17 cells to the site of inflammation. CXCL1, CXCL6, and CXCL10 have chemotactic activity for neutrophils and are involved in CD and UC.<sup>77</sup> However, due to the limited sample size, these candidate proteins need to be validated in larger cohorts to assess their potential as biomarkers for IL23-CAR Treg therapy.

Taken together, our results show IL23R-CAR Treg therapy renders a promising treatment of CD, with the potential long-term benefits of immune tolerance, that warrants further clinical investigation.

## Funding

This work was supported by Sangamo Therapeutics. Data have been generated as part of the routine work of Sangamo Therapeutics.

## Conflict of Interest

All authors are current or former employees of Sangamo Therapeutics. Sangamo Therapeutics has filed patent applications (PCT/EP2019/059590 and PCT/US2022/035028) covering the technology described in this paper.

## Acknowledgments

We are grateful to patients and volunteers who contributed blood and biopsy samples to this study. We thank Pr. Xavier Hebuterne, Dr. Nadia Arab, Elise Mai, Claire Chapman, the study team at Nice Hospital, and the clinical operation team at Sangamo UK for collaborating on the phase 0 study. We also thank Caroline Jeanneau and Coralie Dupont for

lentiviral production, Claire Gendrin and Irene Marchetti for CAR screening, Papa Babacar Fall and Joanne Salhab at the animal facility for excellent care of the mice, Jason Fontenot for scientific advice and Gillian Atkinson and Katharina Schreeb for critical reading of the manuscript.

## Author Contributions

Y.C., M.D., L.B., C.D., T.A., D.F., M.D.L.R., and J.G.D. contributed to the conception and design of the study. Y.C., M.D., L.B., S.R., M.A., C.N., G.L., A.L., G.S., S.B., A.M., A.D., J.F., and S.D.L.F.D.B. performed the experiments. All authors analyzed and/or interpreted the data. Y.C. and J.D.G. wrote the first draft of the manuscript. Y.C., M.D., L.B., S.S., C.D., T.A., D.F., M.D.L.R., and J.G.D. contributed to specific sections and the revision of the manuscript. J.G.D. and M.D.L.R. supervised the study.

## Data Availability

The data underlying this article cannot be shared publicly due to the privacy of individuals that participated in the study. The data will be shared on reasonable request to the corresponding author.

## Supplementary Data

Supplementary data are available online at ECCO-JCC online.

## References

- Colombel JF, Narula N, Peyrin-Biroulet L. Management strategies to improve outcomes of patients with inflammatory bowel diseases. *Gastroenterology* 2017;152:351–61.e5.
- Noor NM, Verstockt B, Parkes M, Lee JC. Personalised medicine in Crohn's disease. *Lancet Gastroenterol Hepatol* 2020;5:80–92.
- Kamada N, Seo SU, Chen GY, Nunez G. Role of the gut microbiota in immunity and inflammatory disease. *Nat Rev Immunol* 2013;13:321–35.
- Baumgart DC, Sandborn WJ. Crohn's disease. *Lancet* 2012;380:1590–605.
- Torres J, Mehandru S, Colombel JF, Peyrin-Biroulet L. Crohn's disease. *Lancet* 2017;389:1741–55.
- D'Haens G. Risks and benefits of biologic therapy for inflammatory bowel diseases. *Gut* 2007;56:725–32.
- Ohkura N, Kitagawa Y, Sakaguchi S. Development and maintenance of regulatory T cells. *Immunity* 2013;38:414–23.
- Izcue A, Coombes JL, Powrie F. Regulatory lymphocytes and intestinal inflammation. *Annu Rev Immunol* 2009;27:313–38.
- Okou DT, Mondal K, Faubion WA, et al. Exome sequencing identifies a novel FOXP3 mutation in a 2-generation family with inflammatory bowel disease. *J Pediatr Gastroenterol Nutr* 2014;58:561–8.
- Maul J, Lodenkemper C, Mundt P, et al. Peripheral and intestinal regulatory CD4+ CD25(high) T cells in inflammatory bowel disease. *Gastroenterology* 2005;128:1868–78.
- Collison LW, Workman CJ, Kuo TT, et al. The inhibitory cytokine IL-35 contributes to regulatory T-cell function. *Nature* 2007;450:566–9.
- Rubtsov YP, Rasmussen JP, Chi EY, et al. Regulatory T cell-derived interleukin-10 limits inflammation at environmental interfaces. *Immunity* 2008;28:546–58.
- Romano M, Fanelli G, Albany CJ, Giganti G, Lombardi G. Past, present, and future of regulatory T cell therapy in transplantation and autoimmunity. *Front Immunol* 2019;10:43.
- Laukova M, Glatman Zaretsky A. Regulatory T cells as a therapeutic approach for inflammatory bowel disease. *Eur J Immunol* 2023;53:e2250007.
- Desreumaux P, Foussat A, Allez M, et al. Safety and efficacy of antigen-specific regulatory T-cell therapy for patients with refractory Crohn's disease. *Gastroenterology* 2012;143:1207–17.e2.
- Goldberg R, Scotta C, Cooper D, et al. Correction of defective T-regulatory cells from patients with Crohn's disease by ex vivo ligation of retinoic acid receptor-alpha. *Gastroenterology* 2019;156:1775–87.
- Voskens C, Stoica D, Rosenberg M, et al. Autologous regulatory T-cell transfer in refractory ulcerative colitis with concomitant primary sclerosing cholangitis. *Gut* 2023;72:49–53.
- Hoffmann P, Eder R, Boeld TJ, et al. Only the CD45RA+ subpopulation of CD4+ CD25 high T cells gives rise to homogeneous regulatory T-cell lines upon in vitro expansion. *Blood* 2006;108:4260–8.
- Canavan JB, Scottà C, Vossenkämper A, et al. Developing in vitro expanded CD45RA + regulatory T cells as an adoptive cell therapy for Crohn's disease. *Gut* 2016;584–94.
- Tarbell KV, Petit L, Zuo X, et al. Dendritic cell-expanded, islet-specific CD4+ CD25+ CD62L+ regulatory T cells restore normoglycemia in diabetic NOD mice. *J Exp Med* 2007;204:191–201.
- Stephens LA, Malpass KH, Anderton SM. Curing CNS autoimmune disease with myelin-reactive Foxp3+ Treg. *Eur J Immunol* 2009;39:1108–17.
- Wright GP, Notley CA, Xue SA, et al. Adoptive therapy with redirected primary regulatory T cells results in antigen-specific suppression of arthritis. *Proc Natl Acad Sci USA* 2009;106:19078–83.
- Elinav E, Adam N, Waks T, Eshhar Z. Amelioration of colitis by genetically engineered murine regulatory T cells redirected by antigen-specific chimeric receptor. *Gastroenterology* 2009;136:1721–31.
- Elinav E, Waks T, Eshhar Z. Redirection of regulatory T cells with predetermined specificity for the treatment of experimental colitis in mice. *Gastroenterology* 2008;134:2014–24.
- Mohseni YR, Tung SL, Dudreuilh C, Lechler RI, Fruhwirth GO, Lombardi G. The future of regulatory T cell therapy: promises and challenges of implementing CAR technology. *Front Immunol* 2020;11:1608.
- Gross G, Waks T, Eshhar Z. Expression of immunoglobulin-T-cell receptor chimeric molecules as functional receptors with antibody-type specificity. *Proc Natl Acad Sci U S A* 1989;86:10024–8.
- Brudno JN, Kochenderfer JN. Chimeric antigen receptor T-cell therapies for lymphoma. *Nat Rev Clin Oncol* 2018;15:31–46.
- Chong EA, Ruella M, Schuster SJ; Lymphoma Program Investigators at the University of Pennsylvania. Five-year outcomes for refractory B-cell lymphomas with CAR T-cell therapy. *N Engl J Med* 2021;384:673–4.
- Neelapu SS, Jacobson CA, Ghobadi A, et al. Five-year follow-up of ZUMA-1 supports the curative potential of axicabtagene ciloleucel in refractory large B-cell lymphoma. *Blood* 2023;141:2307–15.
- Louis CU, Savoldo B, Dotti G, et al. Antitumor activity and long-term fate of chimeric antigen receptor-positive T cells in patients with neuroblastoma. *Blood* 2011;118:6050–6.
- MacDonald KG, Hoeppli RE, Huang Q, et al. Alloantigen-specific regulatory T cells generated with a chimeric antigen receptor. *J Clin Invest* 2016;126:1413–24.
- Muller YD, Ferreira LMR, Ronin E, et al. Precision engineering of an anti-HLA-A2 chimeric antigen receptor in regulatory T cells for transplant immune tolerance. *Front Immunol* 2021;12:686439.
- Proics E, David M, Mojibian M, et al. Preclinical assessment of antigen-specific chimeric antigen receptor regulatory T cells for use in solid organ transplantation. *Gene Ther* 2023;30:309–22.
- Tenspolde M, Zimmermann K, Weber LC, et al. Regulatory T cells engineered with a novel insulin-specific chimeric antigen receptor as a candidate immunotherapy for type 1 diabetes. *J Autoimmun* 2019;103:102289.
- Radichev IA, Yoon J, Scott DW, Griffin K, Savinov AY. Towards antigen-specific Tregs for type 1 diabetes: Construction and

- functional assessment of pancreatic endocrine marker, HPi2-based chimeric antigen receptor. *Cell Immunol* 2020;358:104224.
36. Fransson M, Piras E, Burman J, et al. CAR/FoxP3-engineered T regulatory cells target the CNS and suppress EAE upon intranasal delivery. *J Neuroinflammation* 2012;9:112.
  37. De Paula Pohl A, Schmidt A, Zhang AH, Maldonado T, Konigs C, Scott DW. Engineered regulatory T cells expressing myelin-specific chimeric antigen receptors suppress EAE progression. *Cell Immunol* 2020;358:104222.
  38. Blat D, Zsigmond E, Alteber Z, Waks T, Eshhar Z. Suppression of murine colitis and its associated cancer by carcinoembryonic antigen-specific regulatory T cells. *Mol Ther* 2014;22:1018–28.
  39. Boardman DA, Wong MQ, Rees WD, et al. Flagellin-specific human CAR Tregs for immune regulation in IBD. *J Autoimmun* 2023;134:102961.
  40. Bolivar-Wagers S, Loschi ML, Jin S, et al. Murine CAR19 Tregs suppress acute graft-versus-host disease and maintain graft-versus-tumor responses. *JCI Insight* 2022;7:e160674. doi:10.1172/jci.insight.160674.
  41. Doglio M, Ugolini A, Bercher-Brayer C, et al. Regulatory T cells expressing CD19-targeted chimeric antigen receptor restore homeostasis in systemic lupus erythematosus. *Nat Commun* 2024;15:2542.
  42. Bastian H, Lounnas-Mourey N, Heimendinger P, et al. Feasibility of manufacture of chimeric antigen receptor-regulatory T cells from patients with end-stage renal disease. *Transl Med Commun* 2023;8:15.
  43. Duerr RH, Taylor KD, Brant SR, et al. A genome-wide association study identifies IL23R as an inflammatory bowel disease gene. *Science* 2006;314:1461–3.
  44. Neurath MF. Targeting immune cell circuits and trafficking in inflammatory bowel disease. *Nat Immunol* 2019;20:970–9.
  45. Ahern PP, Schiering C, Buonocore S, et al. Interleukin-23 drives intestinal inflammation through direct activity on T cells. *Immunity* 2010;33:279–88.
  46. Elson CO, Cong Y, Weaver CT, et al. Monoclonal anti-interleukin 23 reverses active colitis in a T cell-mediated model in mice. *Gastroenterology* 2007;132:2359–70.
  47. Yen D, Cheung J, Scheerens H, et al. IL-23 is essential for T cell-mediated colitis and promotes inflammation via IL-17 and IL-6. *J Clin Invest* 2006;116:1310–6.
  48. Buonocore S, Ahern PP, Uhlig HH, et al. Innate lymphoid cells drive interleukin-23-dependent innate intestinal pathology. *Nature* 2010;464:1371–5.
  49. Teng MW, Bowman EP, McElwee JJ, et al. IL-12 and IL-23 cytokines: from discovery to targeted therapies for immune-mediated inflammatory diseases. *Nat Med* 2015;21:719–29.
  50. Fedchenko N, Reifnath J. Different approaches for interpretation and reporting of immunohistochemistry analysis results in the bone tissue - a review. *Diagn Pathol* 2014;9:221.
  51. Krajewska M, Krajewski S, Epstein JI, et al. Immunohistochemical analysis of bcl-2, bax, bcl-X, and mcl-1 expression in prostate cancers. *Am J Pathol* 1996;148:1567–76.
  52. Bolger AM, Lohse M, Usadel B. Trimmomatic: a flexible trimmer for Illumina sequence data. *Bioinformatics* 2014;30:2114–20.
  53. Dobin A, Davis CA, Schlesinger F, et al. STAR: ultrafast universal RNA-seq aligner. *Bioinformatics* 2013;29:15–21.
  54. Liao Y, Smyth GK, Shi W. an efficient general purpose program for assigning sequence reads to genomic features. *Bioinformatics* 2014;30:923–30.
  55. Love MI, Huber W, Anders S. Moderated estimation of fold change and dispersion for RNA-seq data with DESeq2. *Genome Biol* 2014;15:550.
  56. Langfelder P, Horvath S. WGCNA: an R package for weighted correlation network analysis. *BMC Bioinf* 2008;9:559.
  57. Chen EY, Tan CM, Kou Y, et al. Enrichr: interactive and collaborative HTML5 gene list enrichment analysis tool. *BMC Bioinf* 2013;14:128.
  58. Dawson NAJ, Rosado-Sanchez I, Novakovsky GE, et al. Functional effects of chimeric antigen receptor co-receptor signaling domains in human regulatory T cells. *Sci Transl Med* 2020;12:eaa3866.
  59. Wardell CM, MacDonald KN, Levings MK, Cook L. Cross talk between human regulatory T cells and antigen-presenting cells: lessons for clinical applications. *Eur J Immunol* 2021;51:27–38.
  60. Mavin E, Nicholson L, Rafez Ahmed S, Gao F, Dickinson A, Wang XN. Human regulatory T cells mediate transcriptional modulation of dendritic cell function. *J Immunol* 2017;198:138–46.
  61. Misra N, Bayry J, Lacroix-Desmazes S, Kazatchkine MD, Kaveri SV. Cutting edge: human CD4+CD25+ T cells restrain the maturation and antigen-presenting function of dendritic cells. *J Immunol* 2004;172:4676–80.
  62. Mezghiche I, Yahia-Cherbal H, Rogge L, Bianchi E. Interleukin 23 receptor: expression and regulation in immune cells. *Eur J Immunol* 2023;54:e2250348.
  63. Raelson JV, Little RD, Ruether A, et al. Genome-wide association study for Crohn's disease in the Quebec founder population identifies multiple validated disease loci. *Proc Natl Acad Sci USA* 2007;104:14747–52.
  64. Ball JA, Clear A, Aries J, et al. Retinoic acid-responsive CD8 effector T cells are selectively increased in IL-23-rich tissue in gastrointestinal GVHD. *Blood* 2021;137:702–17.
  65. Martin JC, Chang C, Boschetti G, et al. Single-cell analysis of Crohn's disease lesions identifies a pathogenic cellular module associated with resistance to anti-TNF therapy. *Cell* 2019;178:1493–508.e20.
  66. Smillie CS, Biton M, Ordovas-Montanes J, et al. Intra- and Inter-cellular rewiring of the human colon during ulcerative colitis. *Cell* 2019;178:714–30.e22.
  67. Frigault MJ, Lee J, Basil MC, et al. Identification of chimeric antigen receptors that mediate constitutive or inducible proliferation of T cells. *Cancer Immunol Res* 2015;3:356–67.
  68. Long AH, Haso WM, Shern JF, et al. 4-1BB costimulation ameliorates T cell exhaustion induced by tonic signaling of chimeric antigen receptors. *Nat Med* 2015;21:581–90.
  69. Weber EW, Maus MV, Mackall CL. The emerging landscape of immune cell therapies. *Cell* 2020;181:46–62.
  70. Lamarche C, Ward-Hartstonge K, Mi T, et al. Tonic-signaling chimeric antigen receptors drive human regulatory T cell exhaustion. *Proc Natl Acad Sci USA* 2023;120:e2219086120.
  71. Lamarthee B, Marchal A, Charbonnier S, et al. Transient mTOR inhibition rescues 4-1BB CAR-Tregs from tonic signal-induced dysfunction. *Nat Commun* 2021;12:6446.
  72. Miyara M, Yoshioka Y, Kitoh A, et al. Functional delineation and differentiation dynamics of human CD4+ T cells expressing the FoxP3 transcription factor. *Immunity* 2009;30:899–911.
  73. Skartsis N, Peng Y, Ferreira LMR, et al. IL-6 and TNFalpha drive extensive proliferation of human tregs without compromising their lineage stability or function. *Front Immunol* 2021;12:783282.
  74. Shevach EM. Mechanisms of foxp3+ T regulatory cell-mediated suppression. *Immunity* 2009;30:636–45.
  75. Vignali DA, Collison LW, Workman CJ. How regulatory T cells work. *Nat Rev Immunol* 2008;8:523–32.
  76. Borg-Bartolo SP, Boyapati RK, Satsangi J, Kalla R. Precision medicine in inflammatory bowel disease: concept, progress and challenges. *F1000Res* 2020;9:F1000 Faculty Rev-54.
  77. Zhong W, Kolls JK, Chen H, McAllister F, Oliver PD, Zhang Z. Chemokines orchestrate leukocyte trafficking in inflammatory bowel disease. *Front Biosci* 2008;13:1654–64.